Multiscale model of the different modes of cancer cell invasion

Marco Ruscone[1,2,3,4] ✉, **Arnau Montagud**[5], **Philippe Chavrier**[6], **Olivier Destaing**[7], **Andrei Zinovyev**[1,2,3], **Emmanuel Barillot**[1,2,3], **Vincent Noël**[1,2,3], **and Laurence Calzone**[1,2,3] ✉

[1]Institut Curie, Université PSL, F-75005, Paris, France
[2]INSERM, U900, F-75005, Paris, France
[3]Mines ParisTech, Université PSL, F-75005, Paris, France
[4]Sorbonne university, Paris
[5]Barcelona Supercomputing Center (BSC), Barcelona, Spain
[6]Institut Curie, PSL Research University, CNRS, UMR 144, Paris, France
[7]Institute for Advanced Biosciences, Centre de Recherche Université Grenoble Alpes, Inserm U 1209, CNRS UMR 5309, France

Mathematical models of biological processes implicated in cancer are built using the knowledge of complex networks of signaling pathways, describing the molecular regulations inside different cell types, such as tumor cells, immune and other stromal cells. If these models mainly focus on intracellular information, they often omit a description of the spatial organization among cells and their interactions, and with the tumoral microenvironment. We present here a model of tumor cell invasion simulated with PhysiBoSS, a multiscale framework which combines agent-based modeling and continuous time Markov processes applied on Boolean network models. With this model, we aim to study the different modes of cell migration through the extracellular matrix by considering both spatial information obtained from the agent-based simulation and intracellular regulation obtained from the Boolean model. Our multiscale model integrates the impact of gene mutations with the perturbation of the environmental conditions and allows the visualization of the results with 2D and 3D representations. The model successfully reproduces single and collective migration processes and is validated on published experiments on cell invasion. *In silico* experiments are suggested to search for possible targets that can block the more invasive tumoral phenotypes.

Multiscale | Cancer | Agent-based model | Invasion

Correspondence: ***marco.ruscone@curie.fr (Institut Curie)***
laurence.calzone@curie.fr (Institut Curie)

1. Introduction

Cancer is the top cause of disease burden in the world according to the World Health Organization (WHO) (1). The severity of cancer is greatly increased by the invasion of cancerous cells into its surrounding environment, through a metastatic process that may end up in the generation of a secondary cancer seeding (2, 3). Cell invasion is a complex multiscale process that requires the coordinated action of entities at the cells' molecular, cellular and population level. In addition, cell invasion is dependent on the interplay between cells and the extracellular environment (4): depending on the proteins being expressed, cells can affect the presence and density of the extracellular matrix (ECM). Likewise, the extracellular environment can constrain the cellular invasion (5, 6): the ECM stiffness and the availability of oxygen or nutrients will affect the intracellular behaviors, and ECM acts as a repository for a variety of different growth factors and matricellular proteins that are released upon ECM modification (7). This complex dynamic system causes a wide array of different invasion behaviors that have been described in different cancers (2, 8–11). They have been categorized in three main invasion modes (12, 13), where cells move either individually, collectively or in streams of cells. Although these terms are arguably arbitrary and their description can be incomplete, notably at the molecular level, they are useful as they simplify and categorize the literature, and they facilitate the study of the molecular mechanisms underlying each mode (12). Single-cell or individual migration is the invasion mode where cell-cell junctions have been lost and cells are free to degrade and roam the ECM (13). Depending on the tissue, this single-cell mode can be further described as amoeboid, where cells have low adhesion force and spherical shapes, or as mesenchymal, where cells have cytoskeletal protrusions, adhesion capabilities and a spindle shape, with elongated morphologies and proteolytic activity toward ECM substrates. Collective migration is the invasion mode where cell-cell adhesions are retained and cells invade as multicellular groups, requiring a certain coordination between cell-cell adhesion and migration (14, 15). This mode has been identified as more aggressive and with higher metastatic potential, especially in circulating tumor cells and breast cancer (16, 17). Trail or multicellular streaming migration is a special case of the single-cell invasion mode where individual cells move one after the other using the same path within the tissue (12). This can be caused by a given chemoattractant or due to local ECM heterogeneities that allows for a path of less friction for cells. Independently of the invasion mode, the first step of cellular invasion is the detachment of cells from its neighboring tumor tissue. The epithelial-to-mesenchymal transition (EMT) is a molecular program that triggers tumor cell invasion in response to environmental signals (18, 19) by detaching cells from its neighbors (13, 20), promoting cell-matrix adhesion and the formation of protrusion at the cell membrane (21, 22) and by secreting matrix metalloproteases (MMPs) that degrade the ECM (23). EMT allows the cell to switch to a more motile phenotype, losing adhesion to neighboring cells and promoting invasiveness at the single cell level by reducing the expression of E-Cadherin (CDH1) and increasing the expression of N-Cadherin (CDH2). This cadherin switch is driven by EMT regulators such as Twist1, Zeb1, Zeb2, Snai1, or Snai2 (24) which activation can be in-

duced by the focal adhesion kinase (FAK) activity, the tyrosine kinase SRC phosphorylation in response to cell-matrix contact (25, 26), RhoGTPAses activity (RhoA, Rac1, Cdc42) (27, 28), or the presence of Transforming Growth Factor Beta (TGF-beta) (29). To study the invasion process that spans many time and spatial scales, multiscale models such as agent-based modeling are ideally suited as they consider agents as surrogate of cells that move, divide, and die, which facilitates the specific description of both intracellular, secretion and microenvironment behaviors (30). Agent-based modeling has been successfully applied to cancer studies (31, 32) and together with the increased capacity provided by the high-performance computing, it is now efficient enough to scale to the tissue-level simulation (33). Some agent-based studies have focused on describing the effect of the pressure and the interactions between the agents and the ECM (34) without considering any intracellular pathways. Other works have combined the agents with partial and ordinary differential equations to describe the gene regulatory networks of intracellular regulations (35). However, one issue with this formalism is that these dynamical models only cover a small part of the biological mechanisms and often require many parameters that need to be fitted with experiments and high computational cost. One way to cope with this limitation is to describe the intracellular regulations with the Boolean formalism, which although providing a less detailed description, requires no or very few parameters (36, 37). In this study, we use PhysiBoSS (38, 39) a software that combines PhysiCell (40), an agent-based modeling framework that integrates interactions between cells, cell types and with the microenvironment, and MaBoSS (41, 42), a tool that relies on stochastic simulations of Boolean intracellular signaling models. PhysiBoSS allows for the combined genetic and environmental perturbations of tumors and inspects their effect at the population level, enabling the study of drug treatments and cellular heterogeneity and their effect on cancer phenotypes. PhysiBoSS is used to describe a novel model of tumor growth that combines a description of the signaling pathways that trigger events leading to an invasive phenotype, focusing on both single-cell and collective features. By varying the parameters of the agent-based model and various intracellular components, the model reproduces the different modes of invasion and provides a tool for the suggestion of potential drug treatments and genetic perturbations that could block or perturb specific invasion modes.

2. Methods

2.1 A multiscale framework combining Boolean models with agent-based models.

The model of the different modes of invasion links two formalisms. With these two formalisms, we provide two levels of description, one at the level of the individual cell with the interplay between the signaling pathways that activate various phenotypes (with MaBoSS), and one at the level of the cell population where cells interact and trigger cell fates depending on their surrounding environment (with PhysiBoSS). The multiscale model presented here combines an intracellular gene regulatory network with several signaling pathways and generic cell-level parameters. The intracellular model represents interactions often deregulated in cancer and is a refinement and extension of already published models of the invasion mechanisms (43, 44).

2.2 MaBoSS, a method and software for simulating Boolean models with a stochastic approach.

MaBoSS is a C++ software for simulating Boolean models using continuous time Markov processes (41, 42). In Boolean models, the variables can take two values, 0 for absent or inactive and 1 for present or active, and the update of these variables is monitored by logical rules that link all the inputs of a node with the logical connectors OR, AND and NOT. Time is discrete and each update of the model states (vectors of all variable values) is considered to be an event. By considering Markov processes onto these Boolean networks, it is possible to include continuous time into this framework through the Gillespie algorithm (45) and by associating transition rates to each node, for both activation and inactivation. This allows us to generate continuous trajectories with a notion of physical time. Details about MaBoSS are available at: https://github.com/maboss-bkmc/MaBoSS-env-2.0 and in (41, 42).

2.3 PhysiBoSS, an add-on of PhysiCell that integrates stochastic simulation of Boolean models.

PhysiBoSS is a multiscale modeling framework, implemented in C++, that combines agent-based modeling of physico-chemical cell-cell and cell-environment interactions with continuous time Markov process generated by Boolean network models to describe the intracellular signaling. The software was developed by integrating MaBoSS into PhysiCell, a physics-based multicellular simulator (40). This software is actively being developed with new features, new ways to visualize the simulation outputs (39) and a refactoring to run on high performance computers (HPC) (46). To facilitate its use, a graphical user interface (GUI) using Jupyter Notebook has been implemented (see supplementary material) (47). The spatial domain is composed of a mesh of voxels (three dimensional pixels). In PhysiBoSS, each agent is considered to be a single cell, able to divide, move, differentiate and interact not only with the microenvironment through uptake and secretion, but also with the surrounding cells through adhesion and repulsion. The software provides the user with several built-in functions and models of the cell cycle and cell death. There is a feedback of variables between the Boolean model and the agent-based model. The intracellular model receives diverse stimuli from the environment by activating a membrane receptor (input) that triggers signaling pathways and molecular interactions, ultimately leading to different cell responses through MaBoSS simulations. These cell fates are represented by phenotypes that, among others, include cell division (by activating the M-type cyclins), cell death (by cleaving the effector caspase 3) and EMT (by switching on the associated transcription factors Zeb1, Zeb2, Snai1, Snai2 or Twist1). Some components can be secreted by the cell, released in the cell environment, which can acti-

vate or inactivate the neighboring cells. These cell fates, in turn, affect different variables and parameters of the agent-based model and of neighboring cells. For instance, the release of MMPs will degrade the ECM, and subsequently free some proteins that will activate the receptors of neighboring cells or the intracellular model can determine the loss of adherence with other neighboring cells and the detachment from the primary tumor.

2.4 Experimental data used to validate the Boolean model.

We selected three publications with images and videos to validate the model. The first one is based on the work of Ilina et al. (48) to explore how different densities of ECM affect the invasion modes. Figure 3 (3) compares the simulated experiments with Figure 2.i of their work, where they used 4T1 breast cancer cell line in 3D collagen matrices of different densities. The second example compares the model to the experimental results of Lodillinsky and colleagues (49). In their work, they observed the regulation of MT1-MMP by upregulating p63 in breast cancer ductal carcinoma in situ (DCIS). The model is able to reproduce images presented in Figure 6 of their publication where they explored the effects of the expression of a shRNA targeting p63 on invasion (immediately or after 2 days), as seen in Figure 3. The configuration for this experiment involves multicellular spheroids of DCIS cells embedded in a 3D type I collagen matrix. Finally, we considered the work of Moitrier et al. (50) where it was shown that a direct intervention on the SRC oncoprotein causes the displaying of some EMT activators in Madin-Darby Canine Kidney cells (MDCK). Their configuration involves a monolayer of MDCK cells that express a light-sensitive version of SRC. Using this approach, they were able to directly modulate the SRC expression using a blue light activation. We compare the results of our simulations with Moitrier's Figure 4.a, as seen in Figure 5 (3). The panel shows the cell flow during collective extrusion upon 48 hours of blue light illumination.

2.5 Model simulation of the experiment.

Mutations or drug treatments are simulated by forcing the value of the corresponding nodes to 0 in the case of an inhibiting mutation (or treatment) and to 1 in the case of an activating mutation (or treatment). We adapted the simulation setups to simulate the published experiments. For instance, to simulate the experiments from Moitrier and colleagues (50), we set up a one-cell thick circle of cells to obtain a monolayer of cells grown on a Petri dish. In addition, we introduced a virtual substrate to represent the blue light activation. At a certain simulation time , the blue light substrate appears in the simulation at the center of the monolayer, as it happens in the experiments.

3. The mathematical model

3.1 The construction of the intracellular model.

The intracellular model builds upon two published models, one of the early steps of metastasis (44) and another of the EMT process (43). The initial model of Cohen and colleagues was built with two inputs: the *ECMenv*, which monitored the status of the extracellular matrix, and *DNA_damage*, which considered DNA alterations that trigger death signals. Four additional inputs were added to account for the presence of *Oxygen*, growth factors (as *GF*), *TGFbeta* and the contact with other neighboring cells (as *Neigh*)(Figure 1. The phenotypes, or outputs of the model now include *CellCycleArrest*, *Apoptosis*, *EMT*, *ECM_adh* (for cell adhesion), *ECM_degrad* (for cell degradation), *Cell_growth* (for the dynamics of the tumor growth) and *Cell_freeze* (for cell motility ability). New genes and pathways were added to properly describe previous and recent experimental observations (see section 3) including mechanisms around p63 (51) and SRC (50, 52). Genes from the Hippo pathway and RhoGTPases, such as YAP1 (53), FAK and RAC1 (27) were also inserted to link external signals (i.e., cell–cell contact, stiffness of the extracellular matrix, and stress signals) and intracellular regulation. In particular, to implement the Hippo pathway and RhoGTPases into the model we introduce an interaction from Selvaggio and colleagues to link YAP1 and SMAD. Currently, the model does not include a mesenchymal to epithelial transition (MET) (54, 55), and a cell in a mesenchymal cell cannot revert its state. Future extensions of the model will develop this aspect. The resulting network encompasses 45 nodes, with 6 input nodes, representing the possible interactions of an individual cell with external elements, and 8 output nodes or read-outs describing the possible observed phenotypes (Figure 1). The model is also provided in SIF format to facilitate the network visualization with Cytoscape (52) (see supplementary material).

3.2 Initial conditions for the simulation of the intracellular model.

The initial conditions of the model were set to represent a given cell's position in the tumor: in the center of the tumor with cells surrounding it (*Oxygen* and growth factors are considered ON), and at the periphery of the tumor in direct contact with the ECM (*Oxygen*, growth factors, *ECM* and *TGFbeta* ON with or without *DNAdamage*) (Figure 2). It is assumed that on the surface of the tumor, cells are more likely to switch from an epithelial to a mesenchymal state, while in the center, they form tight cell junctions preventing movement. For the inner tumor cell conditions, the simulation with MaBoSS shows a high proportion of cells with *Cell_freeze* and *Cell_growth* phenotypes, corresponding to an increase in the tumor mass without signs of invasion (Figure 2A). Instead, activation of *DNA_damage* leads to the activation of the apoptotic pathway (see Supplementary Material). The pressure due to cell crowding activates the *DNA_damage* node, which leads to the secretion of MMPs and the remodeling and degradation of ECM (56, 57). In the absence of DNA damage, a high probability of cells with the *EMT/Migration/ECM_adh* phenotypes is observed, corresponding to a high invasive potential. This is also true in the absence of oxygen and growth factor (see Supplementary Material). The presence of DNA damage inhibits *EMT* while

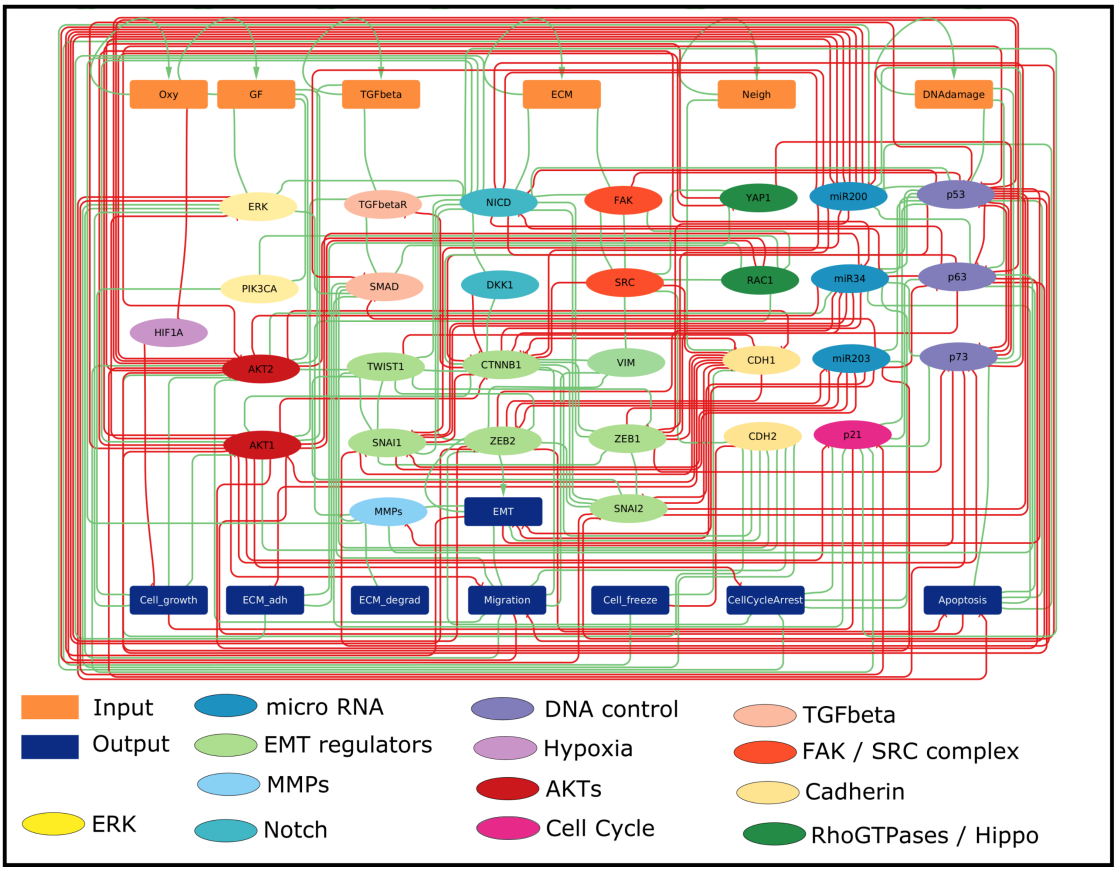

Fig. 1. Influence network of the intracellular model. Rectangular orange nodes represent inputs, rectangular blue nodes represent outputs (or phenotypic read-outs). Ellipsoid nodes are genes or proteins that participate in the signaling pathways listed in the legend: miRNA, Notch, MMPs, DNA control, Hypoxia, Cell Cycle, AKTs, FAK/SRC complex, Rho,GTPase/Hippo, and MAPK pathways, Cadherins, and EMT regulators.

promoting secretion of MMPs (Figure 2C). The combination of the absence of GF and DNA damage leads to an apoptotic state (see Supplementary Material).

Readers can simulate different combinations of initial states using our dedicated Jupyter notebook (supplementary material) and in the GitHub repository https://github.com/sysbio-curie/Invasion_model_PhysiBoSS.

3.3 Defining an agent-based model setup that allows for the integration of the intracellular model.

At the beginning of the simulation, the tumor is represented as a spheroid composed of cancer cells in an epithelial state, surrounded by the ECM. The oxygen can freely diffuse into the microenvironment towards the center of the spheroid, while TGFbeta is encapsulated into the ECM. In the model, oxygen is needed for both cellular respiration and as a triggering signal for the cells' motility. Oxygen can freely diffuse in the environment and is uptaken by the cells. When the internalized value of the oxygen is above a threshold (*oxygen_necrotic_threshold*), the *Oxygen* node of the intracellular model is set to ON. The extracellular matrix (ECM) is defined as a static substrate, i.e., not characterized by a diffusion coefficient and without any decay that prevents the cells from moving across it. It is only when the cells have acquired the appropriate phenotype (*ECM_degrad* and *Migration* active) that they can trigger the invasion process. Secondly, the ECM contains a certain amount of TGFbeta, which is released when the cell degrades the ECM beyond a certain threshold. We fitted this threshold to reproduce experimental data of section 3. It is possible to further explore the model behaviors using different threshold values, however this parameter does not seem to affect the different modes of invasion. When ECM is degraded, TGFbeta becomes accessible to the neighboring cells that initiate its uptake. The presence of oxygen and TGFbeta in the microenvironment, if above a certain threshold, can trigger the activation of the corresponding input node (*TGFbeta*, *Oxy*) in the intracellular model. The ECM input node is triggered when a cell has more contact with the ECM than a user-defined threshold. This value is stored into the variable ecm_contact and is based on the amount of overlap between the cell and the voxel. The intracellular node *Neigh* is the readout for cell-cell contact. In order to quantify cellular contact, the distance between neighboring cells is stored into a variable of the environment *cell_contact* and corresponds to the percentage of their overlapping cell radii. This measure is calculated as follows:

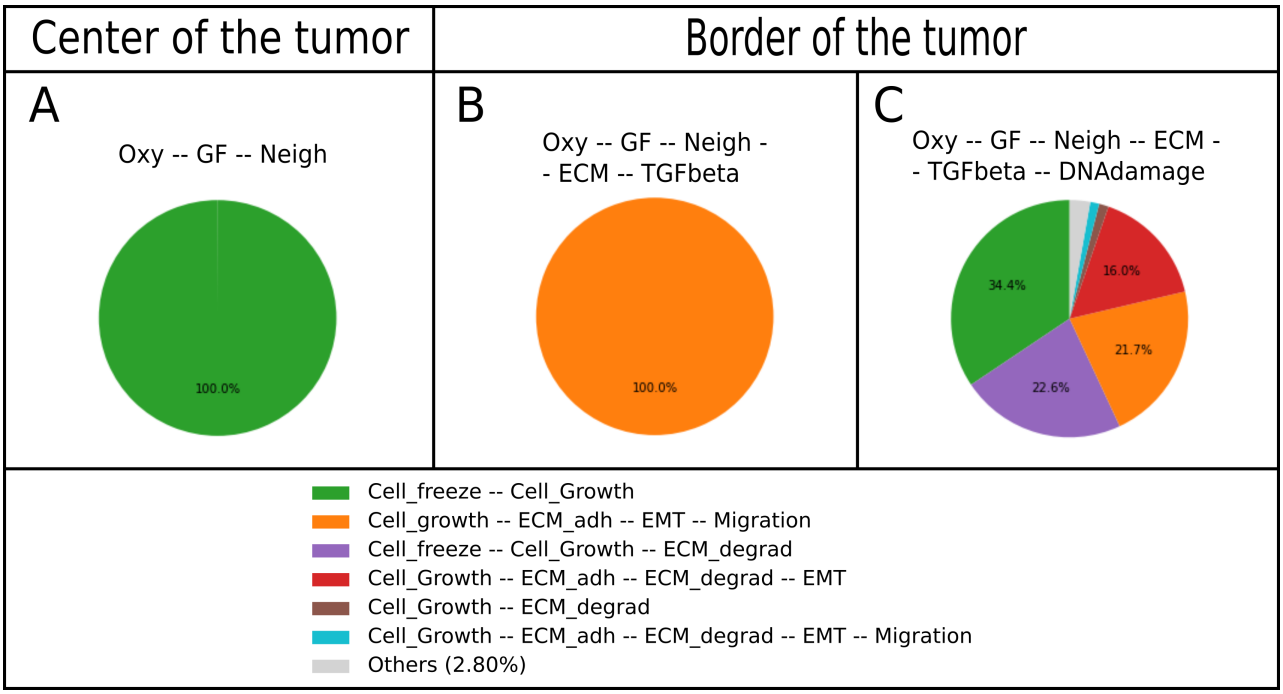

Fig. 2. Asymptotic solutions of the MaBoSS model depicted as pie charts and representing the proportion of cells in a state (i.e., phenotype). Two conditions are simulated: (A) at the center of the tumor with the presence of oxygen, growth factors and in contact with other cells, and with the same conditions but (B) at the border of the tumor, in contact with ECM and exposed to TGFbeta, and (C) with DNA damage.

$$\text{Cellular contact} = \sum_{n=1}^{N} \frac{d_i}{R}$$

where d_i is the distance between a cell and its neighbor i among the total of N neighbors, and R is the radius of a cell. This value is compared to *cell_cell_contact_threshold* thresholds to set *Neigh*'s value. To simulate DNA damage, we consider the physical stress that the cells at the border of the tumor have when they are pushed against the ECM barrier, suffering high nuclear pressure. We represent this pressure as an overlap (distance) between the nucleus radius of the agents and the voxel containing the ECM. When this overlap reaches a given threshold (*DNA_damage_threshold* = 0.8), it triggers the *DNA_damage* node. Similarly, the outputs of the model are usually activated by a combination of active nodes and are connected to specific functions inside each agent. The *Apoptosis* node triggers the apoptotic death model of PhysiCell. *Migration* changes the direction of the motility of the cells, from a random walk to a chemotaxis movement towards the highest concentration of nutrients (represented by oxygen). As *Migration* is activated, the internal variable of the cell *pmotility* increases. This variable changes the length of motility so that the more a cell migrates, the more the displacement of this cell increases at each new step in the simulation. EMT is a read-out in the model, considered as a necessary early step for cell invasion that modifies some mechanical aspects of the agent: once activated, it impacts the *padhesion* variable that indicates the percentage of cell adhesion with neighboring cells. *EMT* value also determines whether a cell forms a cluster with neighboring cells or not, a phenomenon that is characterized by a hook-like adhesion. The formed cluster is disbanded if: 1) *padhesion* is below a certain threshold, simulating the lack of cell junctions by the E-cadherins, or 2) an external mechanical force causes the separation of the cluster. The node *ECM_adh*, that accounts for the junction between the cell and the ECM activates a function that increases the amount of integrins in the agent. The node *ECM_degrad* monitors the secretion of the metalloproteases (MMPs), enzymes that allow the cells to degrade the ECM and hence start invasion. In the model ECM_degrad triggers the uptake rate of ECM substrates based on the amount of integrins displayed by a cell, reducing the density of the ECM value in the target voxel and facilitating the cell's movement through it.

3.4 Impact of the parameter values on the different modes of invasion.

The different modes of invasion depend on the values of a set of parameters listed in the supplementary file. These parameters correspond to biophysical mechanisms that are very difficult to infer from experiments. We propose a set of parameter values in order to simulate the different invasion modes, trying to qualitatively reproduce the experimental images (section 3). To study the impact of the main parameter values, we performed a sensitivity analysis on a subset of 7 parameters, those that cause the simulation to switch from one mode of invasion to another. For each parameter, we select a range of different values (Table 1) and run 50 replicates for each. By modifying their value, we are able to modulate the presence of single cells and cells migrating in clusters (Supplementary file). These 7 parameters were: *cell_ecm_repulsion, epith_cell_attach_threshold, mes_cell_detach_threshold, cell_cell_contact_threshold,*

cell_ecm_contact_threshold, migration_bias and *migration_speed*.

Single cell migration. Single cell migration occurs when a cell has lost the cell junctions with the surrounding cells and starts the invasion process by itself. The parameter *migration_bias* determines the stochasticity of the movement of mesenchymal cells. The higher its value, the less stochastic the movement is. From the results of the sensitivity analysis, it is possible to note a significant increase in the number of single cells with values of *migration_bias* higher than 0.7: with less noise in their movement, the cells reduce their probability to meet others and to form clusters. A similar result is shown for the *migration_speed* parameter. Increasing the speed for mesenchymal cells leads to an increase in the amount of migrating single cells. The number of single cells grows linearly from a *migration_speed* value of 0.3 to 0.8(SuppMat, figure S5). In biological terms, this leads us to say that the more motile a cell is, the less likely it will form a cluster. The range over which to vary the threshold value for *cell_ecm_contact_threshold* and *cell_cell_contact_threshold* was calculated based on the maximum compression reached between cell/cell and cell/ECM. The analysis on the *cell_ecm_contact_threshold* did not show an impact on the migration mode but on the amount of invasion in general. For values superior to 0.5, we observe a drop of the migrating cells, while for inferior values, the ratio between single cells and cells in clusters remains constant. As for the *cell_cell_contact_threshold*, the model proved to be very robust, showing no significant impact on the amount or mode of invasion. The parameters *epith_cell_attach_threshold* and *mes_cell_detach_threshold*, are involved in the process of junction formation between cells in a cluster. We varied these two parameters independently. The former showed no significant change in the invasion modes, while the latter showed an increase in the amount of single cell migration for values between 0.001 and 0.075 but remained constant for higher values. For both parameters, the ratio between single cells and cells in clusters remains constant. Finally, the parameter *cell_ecm_repulsion* modulates the force of repulsion of the ECM that prevents the cells from moving across a voxel full of ECM and maintains them confined within the spheroid. The results of the analysis shows a significant drop in the amount of migrating single cells for values of repulsion higher than 20. For values between 5 and 20, the amount of single cells is constant and significantly higher than the number of cells in clusters. This is due to the fact that for low repulsion values, the cells can reach the ECM voxel more easily, and, with this contact, are able to change to a mesenchymal phenotype before developing cell-cell adhesion and junction.

Collective cell migration. Collective migration can happen when one of two dynamical features appear: (1) a group of epithelial cells go through EMT and start degrading a specific area of the ECM without developing cell junctions before migrating along extracellular boundaries in an uncoordinated collective movement (48); or (2) a group of mesenchymal cells surrounding a small cluster of epithelial cells detach themselves from the main body of the tumor, thus, when epithelial cells have cell junctions with other mesenchymal cells which push them through the ECM. The parameters *migration_bias* and *migration_speed* affect the number of cells in clusters in a similar way as with single cell migration. We observed that the percentage of cells in clusters is higher (around 60% SuppMat figure S4 and S5) than single cells for values of *migration_bias* between 0.3 and 0.75. For values higher than 0.75, the number of cells in clusters rapidly decreases, leaving space for the formation of single cells. For values of *migration_speed* between 0.3 and 0.6, the percentage of cells in clusters decrease from 65% to 55% (Figures S4 and S5 in Supplementary material). For values higher than 0.6, the ratio between single cells and cells in clusters remains almost constant around 50%. As in the previous case, *cell_ecm_contact_threshold* did not show an impact on the migration modes but on the amount of invasion in general. For values superior to 0.5, we observe once again a drop of the migrating cells, while for inferior values, the ratio between single cells and cells in clusters remains constant. The parameter *cell_cell_contact_threshold*, shows a robust behavior with no observable impact on the invasion modes. The thresholds for the formation and disruption of junctions in the clusters impact very moderately the size or the number of clusters. Both for *epith_cell_attach_threshold* and *mes_cell_detach_threshold*, the ratio between single cells and cells in clusters remains constant around 50% showing high robustness (Figures S1 and S2 in Supplementary material). Compared to the migrating single cells, the parameter *cell_ecm_repulsion* has a similar effect on the formation of clusters but with less impact. We observed a drop in the total number of migrating cells in clusters, but much smaller than the one for the single cells. This builds up on the idea that an ECM with high confinement potential favors the formation of migrating clusters.

4. Validation of the model by reproducing migration experiments

In order to validate the model, we successfully reproduced experimental observations reported in three studies: the first one shows the role of the ECM in the different modes of invasion, the second one focuses on the secretion of MMPs through the modification of p63 (49) and the third one on the local activation of SRC which promotes the formation of protrusions leading to collective migration (50). These applications show how interventions to the intracellular or extracellular mechanisms of the cell can affect the behavior of the tumor growth and invasion. The model can then suggest means to interfere with these behaviors, as it is suggested for two of the examples.

4.1 Cell adhesion and density changes in the ECM regulate modes of invasion.

The first example explores the role of the ECM without any modification of the intracellular model. The model is able to reproduce images from data that were not used to build

Parameters	Description	Range
cell_ecm_repulsion	regulates the amount of repulsion between cell and ECM	5 < **15** < 40
epith_cell_attach_threshold	changes the activation threshold needed to attach cells in cluster with cell junction	0.001 < **0.05** < 1
mes_cell_detach_threshold	change the activation threshold needed to detach cells in cluster with cell junction	0.001 < **0.03** < 1
cell_cell_contact_threshold	changes the activation threshold of the value cell_contact needed to trigger the *Neigh* node	0.01 < **0.3** < 3.5
cell_ecm_contact_threshold	changes the activation threshold of the value ecm_contact needed to trigger ECM node	0.001 < **0.05** < 1
migration_bias	changes the value of migration bias for cells with Migration node active	0.5 < **0.85** < 1
migration_speed	changes the value of migration speed for cells with Migration node active	0.3 < **0.7** < 1

Table 1. List of the 7 parameters studied in the sensitivity analysis. For each parameter, we focused on a range of values, picked several values in it, ran 50 simulations for each parameter set and ended up selecting the number in bold (see Supplementary material).

the model. In a recent study, Ilina and colleagues (48) have shown how modifying the ECM density and uniformity affects the migration modes. The experiments were performed on the 4T1 breast cancer cell line, with partial expression of CDH1. The authors observed single cell detachment for low and medium density of the collagen, the experimental proxy of the ECM. In highly dense collagen, single cell invasion was no longer observed. We tested the impact of changing the density of the ECM with our model by changing the value of the parameter *ECM_density*. In a uniform and highly dense ECM (*ECM_density* = 0.8), we confirm low single cell detachment and uncoordinated collective invasion (Figure 3A and B, right panels). This is due to cells at the border of the tumor going through EMT, losing cell-junction adhesion, but remaining confined in the ECM. We further applied a uniform random distribution in the composition of the ECM of the voxels to simulate non-uniform low density ECM (0.1<ECM_density < 0.5). In this condition, we observed a high rate of single cell detachment as reported in the experiments (Figure 3A and B, left panels). The model was able to reproduce both experimental observations and confirmed the role of the ECM in the types of migration that can occur during the early metastatic process.

4.2 Simulation of p63/MT1-MMP axis is required for in situ to invasive transition.

Lodillinsky and colleagues observed that, in basal-like breast cancer, the secretion of MT1-MMP and subsequent cell migration, was strictly linked to the up-regulation of p63 (49). It was shown in this study that the contact of cells with the ECM increased the level of an isoform of p63, Δp63 and as a consequence of MT1-MMP. Through the inhibition of p63, they noticed a strong decrease in the MT1-MMP level, thereby decreasing the process of invasion. The over-expression of MT1-MMP instead reestablished the invasive capacity of p63 depleted cells (Figure 4, top panel). In this example, a modification of the intracellular model shows an impact at the population level. The node *MMPs* of the model accounts for a set of matrix metalloproteases consisting of MT1-MMP (MMP14), MMP13 and MMP2 (23) and its activity is regulated by Notch, SMAD, RAC1, p73 and p63 (see Supplementary Material for more details about the regulations). We first simulated the full inhibition of *p63* (setting the node to 0) in conditions that would activate the migration process (*Oxygen*=1, Growth_factor=1, Neighbor=1, ECM=1, TGFbeta=1, DNAdamage=0). In this simulation, the activation of MMPs was absent, blocking the invasive capacity of the cells and confining the tumor (Figure 4 low panel). When p63 is overexpressed, and as a consequence MMPs are over-activated, the cells are able to degrade the ECM, allowing the tumor to expand and grow (Figure 4) as it is observed in the initial experiment. Here again, the model was able to mimic experimental observations. We notice that the inhibition of p63 does not block the EMT activation. In this scenario, the cells are still able to shift to a mesenchymal state, to grow and to divide. On the other hand, overexpression of p63 in the simulation promotes ECM degradation but blocks EMT transition, allowing tumor expansion but not single or collective migration as was reported by (49). To further explore this scenario, we searched for an additional mutation that could stop invasion in the p63/MMPs over-expression condition. We initially performed a sensitivity analysis of the intracellular model which consisted in automatically deleting and over-expressing all the nodes of the network (see Supplementary Materials), and selected ERK knock-out, which affects the expression of p21 and the phenotype *Cell_growth*, *Apoptosis* and *Migration*. We simulated the p63/MMPs conditions first, without the mutation, and we then introduced the knock-out halfway of the simulation. ERK knock-out caused the triggering of apoptosis in almost all the cells completely stopping the invasion process. Interestingly, the knock-out of ERK without p63 overexpression only caused a small percentage of cells to go to apoptosis without stopping the invasion process.

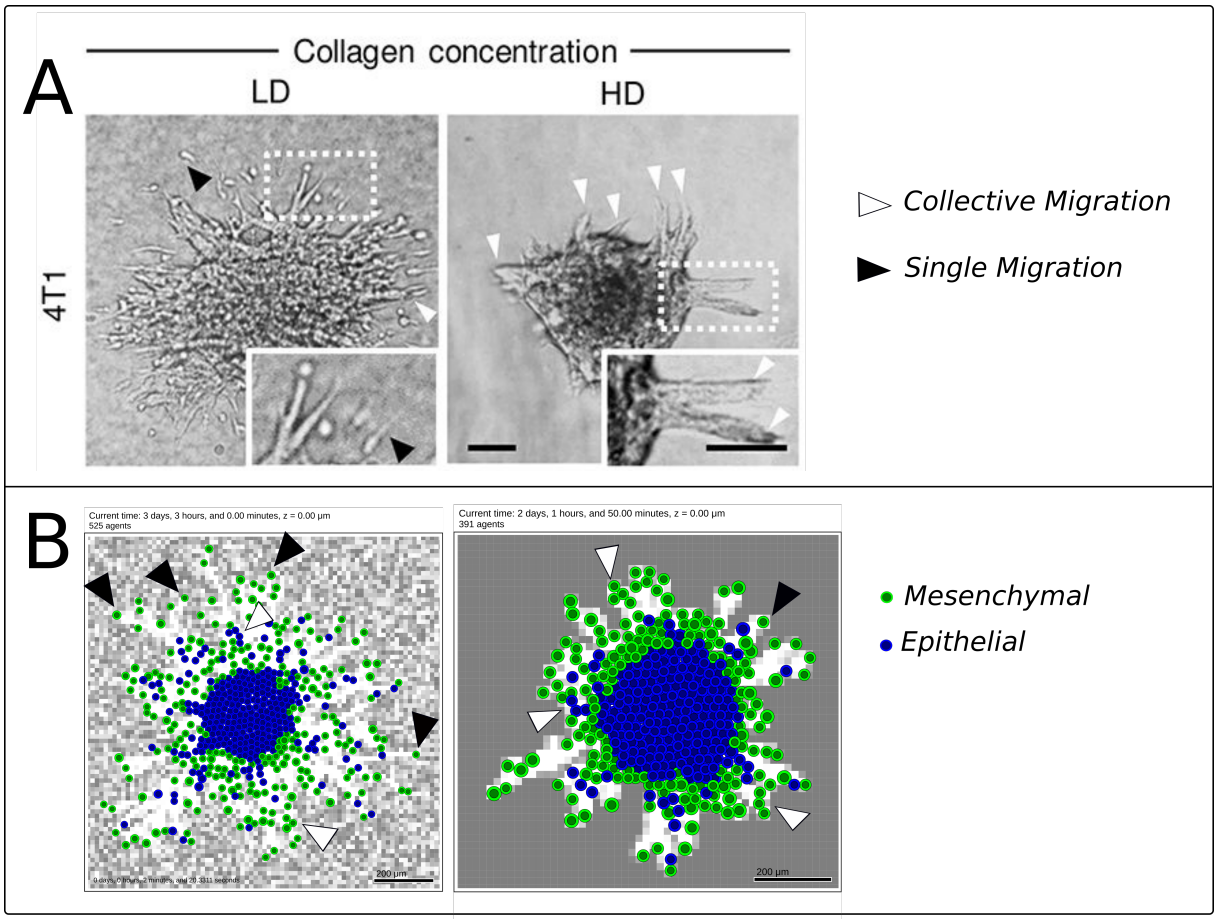

Fig. 3. [Waiting for permission for figure use] Single vs. collective migration observations when varying ECM density and uniformity. (A) experimental observations in response to different ECM density (in uniform (right) and non-uniform conditions, reproduced from (48). (B) Model simulations of the uniform and high density ECM (right) and non-uniform low density ECM (left).

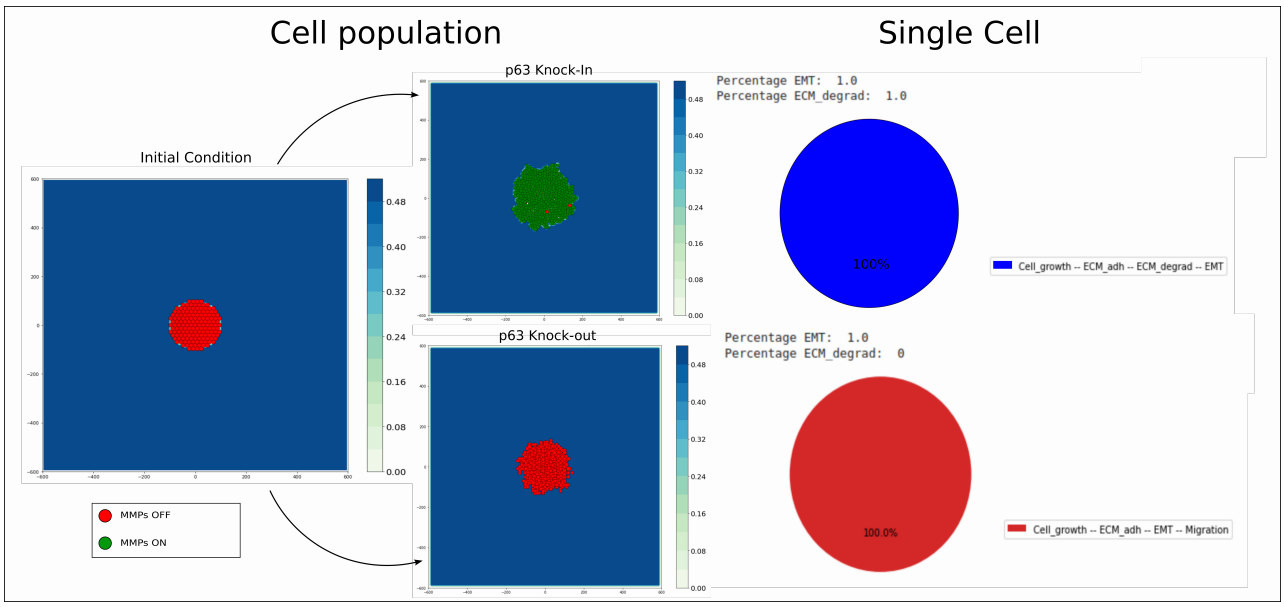

Fig. 4. Reproduction of the p63 knock-in/knock-out experiment from (49). The initial conditions are the same for both simulations. In p63 overexpression condition, it is possible to verify a direct up-regulation of MMPs, leading to a ECM degradation phenotype. This is verified at the single cell level and is interpreted at the cell population level as tumor expansion. In p63 knock-out condition, it is possible to verify a down-regulation of MMPs, that lead to the inhibition of the ECM degradation phenotype. This is also verified at the single cell level and is interpreted at the cell population as tumor confinement.

4.3 Simulation of local light-activation of the SRC oncoprotein in an epithelial monolayer promotes collective extrusion.

Moitrier et al. used a synthetic light-sensitive version of

SRC to trigger its activity upon light activation (50). They subjected a monolayer of cells to intermittent blue light to induce a spatially-constrained activation of the pro-invasive SRC protein and correlated this with the formation of extruded cells that remain cohesive. We adapted the model to simulate this experimental setting (see Methods). In the intracellular model, the SRC oncoprotein regulates the activity of CTNNB1 and CDH2 (58), CDH1 (43) and the production of vimentin (VIM) (59). SRC is activated by focal adhesion kinase (FAK). Upon activation of the blue light, the affected cells start to develop a migratory phenotype similar to that of cells in contact with the ECM. SRC activation triggers the disgregation of cell junctions and EMT, pushing the cells to migrate towards the source of oxygen. The layer of epithelial cells surrounding the cells that have acquired the EMT phenotype confines them and favors the formation of aggregates that try to free themselves by pushing these EMT-like cells outwards, leading to a phenomenon of collective migration (Figure 5). We extended the study by testing the effect of SRC overexpression on the whole tumor. As expected, it caused a burst of invasion, speeding up the formation of both clusters and migrating single cells. As in the previous example, we searched for a way to limit or even suppress the metastasis formation in these conditions. We first tried to stop the activation of the *ECM_degradation* phenotype through a knock-out of *p63*, which was insufficient to inhibit MMPs activation. After performing a sensitivity analysis of the intracellular model, we targeted the ERK gene. As in the previous example, we introduced an inhibitory mutation of ERK halfway through the simulation, which stopped the tumor progression not by promoting apoptosis, but rather by inhibiting the cell movement and cell cycle.

4.4 Simulation of drug candidates that can block migration.

Apart from reproducing three independent studies, the model can also be used as a tool to explore the mechanisms of the cell migration process and as a means to revert invasive phenotypes or prioritize possible points of intervention and drug treatments by performing *in silico* experiments. We tested possible drug candidates that could block migration in conditions where cells have already undergone EMT and have started to invade the surrounding ECM. As a result of a systematic search for single and combined drug treatments, we found that overexpressing the activity of *CTNNB1* (forcing its value to 1) would not prevent tumor growth but would greatly limit the invasive capacity (see Supplementary Material, Figure S2). We tested this hypothesis by introducing an overexpression mutation both at the beginning and halfway through the simulation. In both cases, the treatment blocked the invasive capacities of the cells, preventing the activation of the node MMPs and, as a result, blocking the ECM degradation process. Identifying drugs that target CTNNB1 or any of its downstream actuators could have the potential of limiting invasion. In fact, there have been proposals for targeting CTNNB1 as the main player in the WNT canonical pathway in breast cancer as with 3,6-dihydroxyflavone in MDA-MB-231 cell line (60), even though many unknowns remain (61). A more extensive list of candidates can be found in the supplementary material (Jupyter notebook "intercellular_model_analysis").

5. Discussion

In this study, we presented a multiscale model that combines spatial cell representation and intracellular signaling to reproduce the different modes of cell invasion using PhysiBoSS. The model proved to be efficient in reproducing *in vitro* experiments and simulating different experimental scenarios. We managed to reproduce two invasion modes: single and collective, thanks to a combination of phenotypes and mechanical interactions with the ECM. This study confirms that tumor invasion is a complex process that benefits from considering both spatial information, interaction with the microenvironment and intracellular representation to properly reproduce cell invasion (62).

One application of this model could be to suggest and anticipate the potential risk of metastasis for patients that have a combination of mutations. Currently, the model includes a reasonable amount of genes to allow for a fast simulation and is able to capture the biological differences between the different modes of invasion. However, to be more precise in the predictions that the model could formulate, more genes and pathways could be included in the future based on the experiments one wishes to reproduce or the patients one wishes to tailor it to (63). The choice of these pathways could be suggested by identifying differentially expressed genes or molecular signatures for patients with high metastatic potential. This could be done through exploring the public patient datasets such as The Cancer Genome Atlas (TCGA) data for which clinical data about tumor invasiveness are provided. The intracellular network can also be further extended with the introduction of more input nodes, representing more stimuli. In future releases of the model, we also plan to include more cell types such as cancer associated fibroblast (CAFs) and T-cells to represent the role of the immune response. In this setting, each cell type will have its own intracellular model and would interact with other cell types according to biologically relevant rules.

The current model has shown its predictive potential but there are several limitations. One of them is that the intracellular model can reproduce the EMT transition, but the commitment to EMT is final and non reversible. Nevertheless, we acknowledge the role of the mesenchymal to epithelial transition (MET) in the metastatis process and will include it in further versions of the model. The second limitation concerns the cost of choosing a proper set of parameters that can reproduce experimental data. While performing the sensitivity analysis, we mainly ran into two problems: 1) the number of parameters to analyze for this model is large and requires many long computations, and 2) we noted a high presence of noise in the results (see section 5 in Supplementary material), even for a large number of simulations per parameter (50 runs for each tested value). This adds up to other computational costs of running PhysiBoSS simulations in a regular laptop. Running a 2D simulation can take a couple of minutes, but

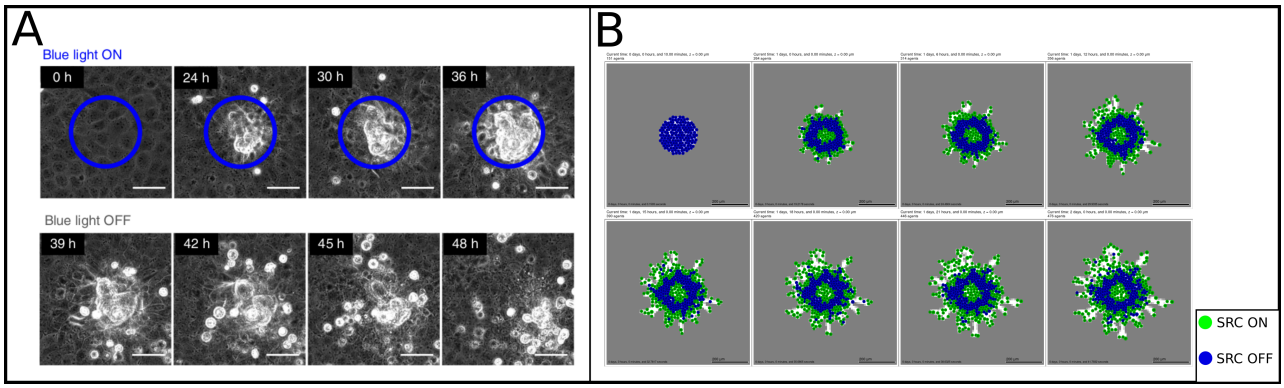

Fig. 5. Reproduction of the SRC experiments. (A) Experimental results of SRC activation at different time points from (50). The blue circle indicates the area of the blue light activation. (B) Model simulation of the SRC experiments. We introduced a substrate that simulate the light in the middle of the epithelial monolayer (blue cells). The substrate virtually interact with the cells with a SRC activating mutation. This cause the cells to undergo EMT and became mesenchymal (green cells) thus trying to migrate and forming aggregates. SRC is also naturally active at the borders of the monolayer, in presence of ECM.

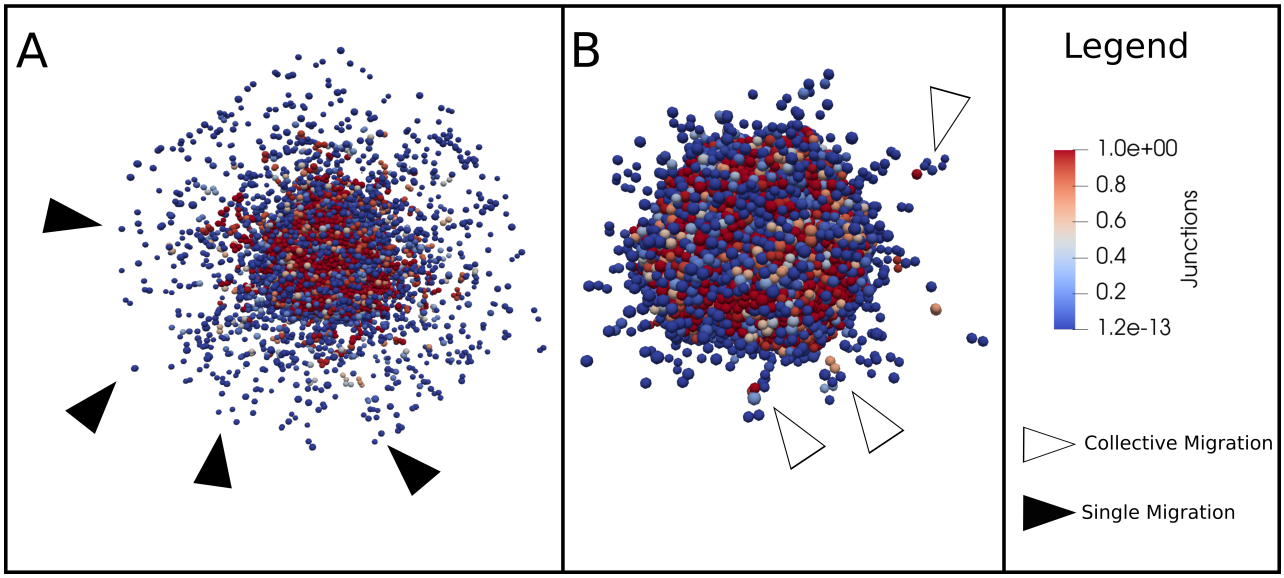

Fig. 6. 3D representation of the simulation. For figures A and B, different values of the parameters have been used to reproduce single (black arrows) and collective cell migration (white arrows). The color bar represents the amount of cell junction used to establish cellular adhesion. (A) cell_ecm_repulsion = 10, cell_junction_attach = 0.5, cell_junction_detach = 0.03, migration_bias = 0.9, migration_speed = 0.8. (B) cell_ecm_repulsion = 15, cell_junction_attach = 0.005, cell_junction_detach = 0.001, migration_bias = 0.8, migration_speed = 0.7.

3D simulations require at least one hour. One way to tackle this issue, especially for very large simulations, is to run them on computer clusters with a high number of cores.

To cope with this parameter exploration issue, which relies on many individual simulations, we plan to explore surrogate models and use them to learn subsets of parameters (64, 65). More specifically, we want to train a machine learning algorithm connecting the inputs (parameter values) and the outputs of PhysiBoSS model, which will act as a surrogate for further parameter optimization. We will compare the output of the surrogate model with *in vitro*/*in vivo* data to find the best combination of parameters which will be tested in a relatively small number of simulations. With sufficiently many new simulations, the surrogate model will be synchronized with the original model by re-training to maintain the correspondence between the two models. Doing so, we hope that the training and the evaluation of large sets of parameter values on the surrogate model will be faster than the evaluation of these sets of parameters using only time-consuming PhysiBoSS simulations.

Finally, we provide a multiscale model that can reproduce experimental observations and that could be used as an exploratory and predictive tool to test hypotheses before performing wet lab experiments. The model is accompanied by the Jupyter Notebook and the Nanohub Tool to facilitate the reproducibility of the results presented here but also to allow users (biologists and/or modelers) to test additional experiments.

ACKNOWLEDGEMENTS
We would like to thank Isabelle Bonnet, Gaëlle Letort and Paul Macklin for inspiration and fruitful discussions.
This work has been partially supported by the European Commission under the PerMedCoE project (H2020-ICT-951773).

6. Supplementary Materials

Below is a list of supplementary file associated to this paper. It is possible to find the supplementary materials at https://github.com/sysbio-curie/

Invasion_model_PhysiBoSS. It is possible to run the model online through the platform Nanohub: https://nanohub.org/resources/invasiongui.

- Supplementary File 1 - Supplementary information

This document contains supplementary information and figures about the model, including a scheme to describe links of the variables of the agent-based model (ABM) model and of the Boolean model (BM), more information about the cell cycle in PhysiBoSS, a complete list of the logical formulae of the BM, a list of the main parameters of the ABM, the CTNNB1 overexpression simulation and the results of the sensitivity analysis.

- Supplementary File 2 - Intracellular_model_analysis

In this jupyter notebook we provide a complete and detailed analysis of the intracellular model that we performed with MaBoSS.

- Supplementary File 3 - Variable_analysis

In this jupyter notebook we provide a more detailed explanation on the evolution of the parameters that linked the intracellular model with the agent-based model.

- maboss_env.yml

This file allows to build an environment using the conda tool, to run the jupyter notebook for the intracellulaer analysis.

- network.sif

This file allows a fast representation of the intracellular model using Cytoscape

- intracellular_model.bnd

This file contains the logical rules of the intracellular signalling network. It is essential in order to run both the model and the Supplementary File 2. It is in a format specific for MaBoSS.

- intracellular_model.cfg

This file contains the initial configuration of the intracellular signalling network. It is essential in order to run both the model and the Supplementary File 2. It is in a format specific for MaBoSS.

7. Bibliography

1. Camilla Mattiuzzi and Giuseppe Lippi. Current Cancer Epidemiology. *Journal of Epidemiology and Global Health*, 9(4):217–222, December 2019. ISSN 2210-6014. doi: 10.2991/jegh.k.191008.001.
2. Felix Weiss, Douglas Lauffenburger, and Peter Friedl. Towards targeting of shared mechanisms of cancer metastasis and therapy resistance. *Nature Reviews Cancer*, 22(3):157–173, March 2022. ISSN 1474-1768. doi: 10.1038/s41568-021-00427-0. Number: 3 Publisher: Nature Publishing Group.
3. Yasir Suhail, Margo P. Cain, Kiran Vanaja, Paul A. Kurywchak, Andre Levchenko, Raghu Kalluri, and Kshitiz. Systems Biology of Cancer Metastasis. *Cell Systems*, 9(2):109–127, August 2019. ISSN 2405-4712. doi: 10.1016/j.cels.2019.07.003.
4. Katarina Wolf, Mariska te Lindert, Marina Krause, Stephanie Alexander, Joost te Riet, Amanda L. Willis, Robert M. Hoffman, Carl G. Figdor, Stephen J. Weiss, and Peter Friedl. Physical limits of cell migration: Control by ECM space and nuclear deformation and tuning by proteolysis and traction force. *Journal of Cell Biology*, 201(7):1069–1084, June 2013. ISSN 1540-8140, 0021-9525. doi: 10.1083/jcb.201210152.
5. Vladimír Čermák, Aneta Gandalovičová, Ladislav Merta, Jitka Fučíková, Radek Špíšek, Daniel Rösel, and Jan Brábek. RNA-seq of macrophages of amoeboid or mesenchymal migratory phenotype due to specific structure of environment. *Scientific Data*, 5:180198, October 2018. ISSN 2052-4463. doi: 10.1038/sdata.2018.198.
6. Yangjin Kim, Hyunji Kang, Gibin Powathil, Hyeongi Kim, Dumitru Trucu, Wanho Lee, Sean Lawler, and Mark Chaplain. Role of extracellular matrix and microenvironment in regulation of tumor growth and LAR-mediated invasion in glioblastoma. *PLOS ONE*, 13(10):e0204865, October 2018. ISSN 1932-6203. doi: 10.1371/journal.pone.0204865. Publisher: Public Library of Science.
7. Boris Hinz. The extracellular matrix and transforming growth factor-beta1: Tale of a strained relationship. *Matrix Biology*, 47:54–65, September 2015. ISSN 0945-053X. doi: 10.1016/j.matbio.2015.05.006.
8. Fabiana Lüönd, Stefanie Tiede, and Gerhard Christofori. Breast cancer as an example of tumour heterogeneity and tumour cell plasticity during malignant progression. *British Journal of Cancer*, 125(2):164–175, July 2021. ISSN 1532-1827. doi: 10.1038/s41416-021-01328-7. Number: 2 Publisher: Nature Publishing Group.
9. Asja Guzman, Rachel C. Avard, Alexander J. Devanny, Oh Sang Kweon, and Laura J. Kaufman. Delineating the role of membrane blebs in a hybrid mode of cancer cell invasion in three-dimensional environments. *Journal of Cell Science*, 133(8):jcs236778, April 2020. ISSN 0021-9533. doi: 10.1242/jcs.236778.
10. Gray W. Pearson. Control of Invasion by Epithelial-to-Mesenchymal Transition Programs during Metastasis. *Journal of Clinical Medicine*, 8(5):646, May 2019. ISSN 2077-0383. doi: 10.3390/jcm8050646. Number: 5 Publisher: Multidisciplinary Digital Publishing Institute.
11. H. Eslami Amirabadi, M. Tuerlings, A. Hollestelle, S. SahebAli, R. Luttge, C. C. van Donkelaar, J. W. M. Martens, and J. M. J. den Toonder. Characterizing the invasion of different breast cancer cell lines with distinct E-cadherin status in 3D using a microfluidic system. *Biomedical Microdevices*, 21(4):101, November 2019. ISSN 1572-8781. doi: 10.1007/s10544-019-0450-5.
12. Peter Friedl and Katarina Wolf. Plasticity of cell migration: a multiscale tuning model. *Journal of Cell Biology*, 188(1):11–19, December 2009. ISSN 0021-9525. doi: 10.1083/jcb.200909003.
13. Peter Friedl and Stephanie Alexander. Cancer Invasion and the Microenvironment: Plasticity and Reciprocity. *Cell*, 147(5):992–1009, November 2011. ISSN 00928674. doi: 10.1016/j.cell.2011.11.016.
14. Peter Friedl and Darren Gilmour. Collective cell migration in morphogenesis, regeneration and cancer. *Nature Reviews Molecular Cell Biology*, 10(7):445–457, July 2009. ISSN 1471-0072, 1471-0080. doi: 10.1038/nrm2720.
15. Samuel A. Vilchez Mercedes, Federico Bocci, Herbert Levine, José N. Onuchic, Mohit Kumar Jolly, and Pak Kin Wong. Decoding leader cells in collective cancer invasion. *Nature Reviews Cancer*, 21(9):592–604, September 2021. ISSN 1474-1768. doi: 10.1038/s41568-021-00376-8. Number: 9 Publisher: Nature Publishing Group.
16. Rachel M. Lee, Michele I. Vitolo, Wolfgang Losert, and Stuart S. Martin. Distinct roles of tumor associated mutations in collective cell migration. *Scientific Reports*, 11(1):10291, December 2021. ISSN 2045-2322. doi: 10.1038/s41598-021-89130-6.
17. Yang Yang, Hongmei Zheng, Yuting Zhan, and Songqing Fan. An emerging tumor invasion mechanism about the collective cell migration. *American Journal of Translational Research*, 11(9):5301–5312, September 2019. ISSN 1943-8141.
18. Jean Paul Thiery, Hervé Acloque, Ruby Y. J. Huang, and M. Angela Nieto. Epithelial-Mesenchymal Transitions in Development and Disease. *Cell*, 139(5):871–890, November 2009. ISSN 0092-8674. doi: 10.1016/j.cell.2009.11.007.
19. Maia Chanrion, Inna Kuperstein, Cédric Barrière, Fatima El Marjou, David Cohen, Danijela Vignjevic, Lev Stimmer, Perrine Paul-Gilloteaux, Ivan Bièche, Silvina Dos Reis Tavares, Giuseppe-Fulvio Boccia, Wulfran Cacheux, Didier Meseure, Silvia Fre, Loredana Martignetti, Patricia Legoix-Né, Elodie Girard, Luc Fetler, Emmanuel Barillot, Daniel Louvard, Andreï Zinovyev, and Sylvie Robine. Concomitant Notch activation and p53 deletion trigger epithelial-to-mesenchymal transition and metastasis in mouse gut. *Nature Communications*, 5:5005, October 2014. ISSN 2041-1723. doi: 10.1038/ncomms6005.
20. Samuel Schmidt and Peter Friedl. Interstitial cell migration: integrin-dependent and alternative adhesion mechanisms. *Cell and Tissue Research*, 339(1):83, November 2009. ISSN 1432-0878. doi: 10.1007/s00441-009-0892-9.
21. Olivier Destaing, Marc R Block, Emmanuelle Planus, and Corinne Albiges-Rizo. Invadosome regulation by adhesion signaling. *Current Opinion in Cell Biology*, 23(5):597–606, October 2011. ISSN 09550674. doi: 10.1016/j.ceb.2011.04.002.
22. Aviv Bergman, John S Condeelis, and Bojana Gligorijevic. Invadopodia in context. *Cell Adhesion & Migration*, 8(3):273–279, May 2014. ISSN 1933-6918, 1933-6926. doi: 10.4161/cam.28349.
23. Robin Ferrari, Gaëlle Martin, Oya Tagit, Alan Guichard, Alessandra Cambi, Raphaël Voituriez, Stéphane Vassilopoulos, and Philippe Chavrier. MT1-MMP directs force-producing proteolytic contacts that drive tumor cell invasion. *Nature Communications*, 10(1):4886, October 2019. ISSN 2041-1723. doi: 10.1038/s41467-019-12930-y. Number: 1 Publisher: Nature Publishing Group.
24. Zhangxiang Zhao, Wenbin Zhou, Yue Han, Fuduan Peng, Ruiping Wang, Ruihan Yu, Chengyu Wang, Haihai Liang, Zheng Guo, and Yunyan Gu. EMT-Regulome: a database for EMT-related regulatory interactions, motifs and network. *Cell Death & Disease*, 8(6):e2872–e2872, June 2017. ISSN 2041-4889. doi: 10.1038/cddis.2017.267.
25. Christof R. Hauck, Datsun A. Hsia, and David D. Schlaepfer. The Focal Adhesion Kinase–A Regulator of Cell Migration and Invasion. *IUBMB Life (International Union of Biochemistry and Molecular Biology: Life)*, 53(2):115–119, February 2002. ISSN 1521-6543, 1521-6551. doi: 10.1080/15216540211470.
26. Adèle Kerjouan, Cyril Boyault, Christiane Oddou, Edwige Hiriart-Bryant, Alexei Grichine, Alexandra Kraut, Mylène Pezet, Martial Balland, Eva Faurobert, Isabelle Bonnet, Yohann Coute, Bertrand Fourcade, Corinne Albiges-Rizo, and Olivier Destaing. Control of SRC molecular dynamics encodes distinct cytoskeletal responses by specifying signaling pathway usage. *Journal of Cell Science*, 134(2):jcs254599, January 2021. ISSN 0021-9533, 1477-9137. doi: 10.1242/jcs.254599.
27. Matteo Parri and Paola Chiarugi. Rac and Rho GTPases in cancer cell motility control. *Cell*

Communication and Signaling, 8(1):23, December 2010. ISSN 1478-811X. doi: 10.1186/1478-811X-8-23.

28. Haiyoung Jung, Suk Ran Yoon, Jeewon Lim, Hee Jun Cho, and Hee Gu Lee. Dysregulation of Rho GTPases in Human Cancers. *Cancers*, 12(5):1179, May 2020. ISSN 2072-6694. doi: 10.3390/cancers12051179.
29. J. Plou, Y. Juste-Lanas, V. Olivares, C. del Amo, C. Borau, and J. M. García-Aznar. From individual to collective 3D cancer dissemination: roles of collagen concentration and TGF-beta. *Scientific Reports*, 8(1):12723, December 2018. ISSN 2045-2322. doi: 10.1038/s41598-018-30683-4.
30. John Metzcar, Yafei Wang, Randy Heiland, and Paul Macklin. A Review of Cell-Based Computational Modeling in Cancer Biology. *JCO Clinical Cancer Informatics*, 3:CCI.18.00069, February 2019. ISSN 2473-4276. doi: 10.1200/CCI.18.00069.
31. Nikolaos Sfakianakis, Anotida Madzvamuse, and Mark A. J. Chaplain. A Hybrid Multiscale Model for Cancer Invasion of the Extracellular Matrix. *Multiscale Modeling & Simulation*, 18 (2):824–850, January 2020. ISSN 1540-3459, 1540-3467. doi: 10.1137/18M1189026.
32. Colin G. Cess and Stacey D. Finley. Multiscale modeling of tumor adaption and invasion following anti-angiogenic therapy. *Computational and Systems Oncology*, 2(1):e1032, 2022. ISSN 2689-9655. doi: 10.1002/cso2.1032. _eprint: https://onlinelibrary.wiley.com/doi/pdf/10.1002/cso2.1032.
33. Arnau Montagud, Miguel Ponce-de Leon, and Alfonso Valencia. Systems biology at the giga-scale: Large multiscale models of complex, heterogeneous multicellular systems. *Current Opinion in Systems Biology*, 28:100385, December 2021. ISSN 2452-3100. doi: 10.1016/j.coisb.2021.100385.
34. Inês G. Gonçalves and Jose Manuel Garcia-Aznar. Extracellular matrix density regulates the formation of tumour spheroids through cell migration. *PLOS Computational Biology*, 17 (2):e1008764, February 2021. ISSN 1553-7358. doi: 10.1371/journal.pcbi.1008764.
35. Dharma Pally, Durjay Pramanik, and Ramray Bhat. An Interplay Between Reaction-Diffusion and Cell-Matrix Adhesion Regulates Multiscale Invasion in Early Breast Carcinomatosis. *Frontiers in Physiology*, 10:790, August 2019. ISSN 1664-042X. doi: 10.3389/fphys.2019.00790.
36. Nicolas Le Novère. Quantitative and logic modelling of gene and molecular networks. *Nature reviews. Genetics*, 16(3):146–158, March 2015. ISSN 1471-0056. doi: 10.1038/nrg3885.
37. Julian D. Schwab, Silke D. Kühlwein, Nensi Ikonomi, Michael Kühl, and Hans A. Kestler. Concepts in Boolean network modeling: What do they all mean? *Computational and Structural Biotechnology Journal*, 18:571–582, January 2020. ISSN 2001-0370. doi: 10.1016/j.csbj.2020.03.001.
38. Gaelle Letort, Arnau Montagud, Gautier Stoll, Randy Heiland, Emmanuel Barillot, Paul Macklin, Andrei Zinovyev, and Laurence Calzone. PhysiBoSS: a multi-scale agent-based modelling framework integrating physical dimension and cell signalling. *Bioinformatics (Oxford, England)*, 35(7):1188–1196, April 2019. ISSN 1367-4811. doi: 10.1093/bioinformatics/bty766.
39. Miguel Ponce-de Leon, Arnau Montagud, Vincent Noël, Gerard Pradas, Annika Meert, Emmanuel Barillot, Laurence Calzone, and Alfonso Valencia. PhysiBoSS 2.0: a sustainable integration of stochastic Boolean and agent-based modelling frameworks. preprint, Systems Biology, January 2022.
40. Ahmadreza Ghaffarizadeh, Randy Heiland, Samuel H. Friedman, Shannon M. Mumenthaler, and Paul Macklin. PhysiCell: An open source physics-based cell simulator for 3-D multicellular systems. *PLOS Computational Biology*, 14(2):e1005991, February 2018. ISSN 1553-7358. doi: 10.1371/journal.pcbi.1005991. Publisher: Public Library of Science.
41. Gautier Stoll, Eric Viara, Emmanuel Barillot, and Laurence Calzone. Continuous time boolean modeling for biological signaling: application of Gillespie algorithm. *BMC Systems Biology*, 6(1):116, August 2012. ISSN 1752-0509. doi: 10.1186/1752-0509-6-116.
42. Gautier Stoll, Barthélémy Caron, Eric Viara, Aurélien Dugourd, Andrei Zinovyev, Aurélien Naldi, Guido Kroemer, Emmanuel Barillot, and Laurence Calzone. MaBoSS 2.0: an environment for stochastic Boolean modeling. *Bioinformatics*, 33(14):2226–2228, July 2017. ISSN 1367-4803. doi: 10.1093/bioinformatics/btx123.
43. Gianluca Selvaggio, Sara Canato, Archana Pawar, Pedro T. Monteiro, Patrícia S. Guerreiro, M. Manuela Brás, Florence Janody, and Claudine Chaouiya. Hybrid Epithelial–Mesenchymal Phenotypes Are Controlled by Microenvironmental Factors. *Cancer Research*, 80(11):2407–2420, June 2020. ISSN 0008-5472, 1538-7445. doi: 10.1158/0008-5472.CAN-19-3147.
44. David P. A. Cohen, Loredana Martignetti, Sylvie Robine, Emmanuel Barillot, Andrei Zinovyev, and Laurence Calzone. Mathematical Modelling of Molecular Pathways Enabling Tumour Cell Invasion and Migration. *PLOS Computational Biology*, 11(11):e1004571, November 2015. ISSN 1553-7358. doi: 10.1371/journal.pcbi.1004571.
45. Daniel T Gillespie. A general method for numerically simulating the stochastic time evolution of coupled chemical reactions. *Journal of Computational Physics*, 22(4):403–434, January 1976. ISSN 0021-9991. doi: 10.1016/0021-9991(76)90041-3. Publisher: Elsevier Inc.
46. Gaurav Saxena, Miguel Ponce-de Leon, Arnau Montagud, David Vicente Dorca, and Alfonso Valencia. BioFVM-X: An MPI+OpenMP 3-D Simulator for Biological Systems. In Eugenio Cinquemani and Loïc Paulevé, editors, *Computational Methods in Systems Biology*, Lecture Notes in Computer Science, pages 266–279, Cham, 2021. Springer International Publishing. ISBN 978-3-030-85633-5. doi: 10.1007/978-3-030-85633-5_18.
47. Randy Heiland, Daniel Mishler, Tyler Zhang, Eric Bower, and Paul Macklin. xml2jupyter: Mapping parameters between XML and Jupyter widgets. *Journal of Open Source Software*, 4(39):1408, July 2019. ISSN 2475-9066. doi: 10.21105/joss.01408.
48. Olga Ilina, Pavlo G. Gritsenko, Simon Syga, Jürgen Lippoldt, Caterina A. M. La Porta, Oleksandr Chepizhko, Steffen Grosser, Manon Vullings, Gert-Jan Bakker, Jörn Starruß, Peter Bult, Stefano Zapperi, Josef A. Käs, Andreas Deutsch, and Peter Friedl. Cell–cell adhesion and 3D matrix confinement determine jamming transitions in breast cancer invasion. *Nature Cell Biology*, 22(9):1103–1115, September 2020. ISSN 1465-7392, 1476-4679. doi: 10.1038/s41556-020-0552-6.
49. Catalina Lodillinsky, Laetitia Fuhrmann, Marie Irondelle, Olena Pylypenko, Xiao-Yan Li, Hélène Bonsang-Kitzis, Fabien Reyal, Sophie Vacher, Claire Calmel, Olivier De Wever, Ivan Bièche, Marie-Lise Lacombe, Ana Maria Eiján, Anne Houdusse, Anne Vincent-Salomon, Stephen J. Weiss, Philippe Chavrier, and Mathieu Boissan. Metastasis-suppressor NME1 controls the invasive switch of breast cancer by regulating MT1-MMP surface clearance. *Oncogene*, 40(23):4019–4032, June 2021. ISSN 0950-9232, 1476-5594. doi: 10.1038/s41388-021-01826-1.
50. Sarah Moitrier, Nastassia Pricoupenko, Adèle Kerjouan, Christiane Oddou, Olivier Destaing, Aude Battistella, Pascal Silberzan, and Isabelle Bonnet. Local light-activation of the Src oncoprotein in an epithelial monolayer promotes collective extrusion. *Communications Physics*, 2(1):98, December 2019. ISSN 2399-3650. doi: 10.1038/s42005-019-0198-5.
51. Ivana Celardo, Alexey Antonov, Ivano Amelio, Margherita Annicchiarico-Petruzzelli, and Gerry Melino. p63 transcriptionally regulates the expression of matrix metallopeptidase 13. *Oncotarget*, 5(5):1279–1289, March 2014. ISSN 1949-2553. doi: 10.18632/oncotarget.1778.
52. Mark Shaaya, Jordan Fauser, Anastasia Zhurikhina, Jason E Conage-Pough, Vincent Huyot, Martin Brennan, Cameron T Flower, Jacob Matsche, Shahzeb Khan, Viswanathan Natarajan, Jalees Rehman, Pradeep Kota, Forest M White, Denis Tsygankov, and Andrei V Karginov. Light-regulated allosteric switch enables temporal and subcellular control of enzyme activity. *eLife*, 9:e60647, September 2020. ISSN 2050-084X. doi: 10.7554/eLife.60647.
53. Chad A. Hall, Runsheng Wang, Jiangyong Miao, Esther Oliva, Xiaoyun Shen, Thomas Wheeler, Susan G. Hilsenbeck, Sandra Orsulic, and Scott Goode. Hippo Pathway Effector Yap is an Ovarian Cancer Oncogene. *Cancer research*, 70(21):8517–8525, November 2010. ISSN 0008-5472. doi: 10.1158/0008-5472.CAN-10-1242.
54. Dianbo Yao, Chaoliu Dai, and Songlin Peng. Mechanism of the Mesenchymal–Epithelial Transition and Its Relationship with Metastatic Tumor Formation. *Molecular Cancer Research*, 9(12):1608–1620, December 2011. ISSN 1541-7786. doi: 10.1158/1541-7786.MCR-10-0568.
55. Gerhard Hamilton and Barbara Rath. Mesenchymal-Epithelial Transition and Circulating Tumor Cells in Small Cell Lung Cancer. In Mark Jesus M. Magbanua and John W. Park, editors, *Isolation and Molecular Characterization of Circulating Tumor Cells*, Advances in Experimental Medicine and Biology, pages 229–245. Springer International Publishing, Cham, 2017. ISBN 978-3-319-55947-6. doi: 10.1007/978-3-319-55947-6_12.
56. Guilherme Pedreira de Freitas Nader, Sonia Agüera-Gonzalez, Fiona Routet, Matthieu Gratia, Mathieu Maurin, Valeria Cancila, Clotilde Cadart, Andrea Palamidessi, Rodrigo Nalio Ramos, Mabel San Roman, Matteo Gentili, Ayako Yamada, Alice Williart, Catalina Lodillinsky, Emilie Lagoutte, Catherine Villard, Jean-Louis Viovy, Claudio Tripodo, Jérôme Galon, Giorgio Scita, Nicolas Manel, Philippe Chavrier, and Matthieu Piel. Compromised nuclear envelope integrity drives TREX1-dependent DNA damage and tumor cell invasion. *Cell*, 184(20):5230–5246.e22, September 2021. ISSN 00928674. doi: 10.1016/j.cell.2021.08.035.
57. Celine M. Denais, Rachel M. Gilbert, Philipp Isermann, Alexandra L. McGregor, Mariska te Lindert, Bettina Weigelin, Patricia M. Davidson, Peter Friedl, Katarina Wolf, and Jan Lammerding. Nuclear envelope rupture and repair during cancer cell migration. *Science*, 352 (6283):353–358, April 2016. doi: 10.1126/science.aad7297. Publisher: American Association for the Advancement of Science.
58. Jianfei Qi, Junfu Wang, Olena Romanyuk, and Chi-Hung Siu. Involvement of Src family kinases in N-cadherin phosphorylation and beta-catenin dissociation during transendothelial migration of melanoma cells. *Molecular Biology of the Cell*, 17(3):1261–1272, March 2006. ISSN 1059-1524. doi: 10.1091/mbc.e05-10-0927.
59. Cheng-Yi Yang, Po-Wei Chang, Wen-Hsin Hsu, Hsuan-Chia Chang, Chien-Lin Chen, Chien-Chen Lai, Wen-Tai Chiu, and Hong-Chen Chen. Src and SHP2 coordinately regulate the dynamics and organization of vimentin filaments during cell migration. *Oncogene*, 38(21): 4075–4094, May 2019. ISSN 1476-5594. doi: 10.1038/s41388-019-0705-x. Number: 21 Publisher: Nature Publishing Group.
60. Jamie N. Anastas and Randall T. Moon. WNT signalling pathways as therapeutic targets in cancer. *Nature Reviews Cancer*, 13(1):11–26, January 2013. ISSN 1474-1768. doi: 10.1038/nrc3419. Number: 1 Publisher: Nature Publishing Group.
61. Emma H. van Schie and Renée van Amerongen. Aberrant WNT/CTNNB1 Signaling as a Therapeutic Target in Human Breast Cancer: Weighing the Evidence. *Frontiers in Cell and Developmental Biology*, 8, 2020. ISSN 2296-634X.
62. Ushasi Roy, Tyler Collins, Mohit K. Jolly, and Parag Katira. Biophysical and Biochemical mechanisms underlying Collective Cell Migration in Cancer Metastasis. *arXiv:2201.07283 [physics, q-bio]*, January 2022. arXiv: 2201.07283.
63. Arnau Montagud, Jonas Béal, Luis Tobalina, Pauline Traynard, Vigneshwari Subramanian, Bence Szalai, Róbert Alföldi, László Puskás, Alfonso Valencia, Emmanuel Barillot, Julio Saez-Rodriguez, and Laurence Calzone. Patient-specific Boolean models of signalling networks guide personalised treatments. *eLife*, 11:e72626, February 2022. ISSN 2050-084X. doi: 10.7554/eLife.72626. Publisher: eLife Sciences Publications, Ltd.
64. Heber L. Rocha, João Vitor de O. Silva, Renato S. Silva, Ernesto A. B. F. Lima, and Regina C. Almeida. Bayesian inference using Gaussian process surrogates in cancer modeling. *Computer Methods in Applied Mechanics and Engineering*, 399:115412, September 2022. ISSN 0045-7825. doi: 10.1016/j.cma.2022.115412.
65. Richard J. Preen, Larry Bull, and Andrew Adamatzky. Towards an Evolvable Cancer Treatment Simulator. *Biosystems*, 182:1–7, August 2019. ISSN 03032647. doi: 10.1016/j.biosystems.2019.05.005. arXiv:1812.08252 [cs].